

# Laser Diagnostics of Inductively Heated Oxygen, Nitrogen and Air Flows

Makoto Matsui\*

*The University of Tokyo, Tokyo, 113-8656, JAPAN*

Georg Herdrich†

*Stuttgart University, Stuttgart, D-70550, GERMANY*  
*The University of Tokyo, Tokyo, 113-8656, JAPAN*

Hiroki Takayanagi‡, Kimiya Komurasaki§, Yoshihiro Arakawa\*\*  
*The University of Tokyo, Tokyo, 113-8656, JAPAN*

and

Monika Auweter-Kurtz††

*Hamburg University, Hamburg, D-20146, GERMANY*

Laser absorption spectroscopy was applied for diagnostics of inductively heated plasma generator IPG3 air and nitrogen flows. Although no absorption signal could be detected in the nitrogen flow, temporal variation of absorption profiles at OI 777.19 nm were measured in the air flow. As a result, the flow properties were found to fluctuate at 300 Hz with the plasma emitted duration of 46%. The specific total enthalpy and degree of dissociation in oxygen and nitrogen were estimated from the deduced total temperature assuming thermochemical equilibrium in the discharge tube. Consequently, the averaged total enthalpy, degree of dissociation in oxygen and nitrogen in the emitted duration time were estimated as 23.5±10.1 MJ/kg, 98% and 44 %, respectively.

## Nomenclature

$A$	= Einstein coefficient, $s^{-1}$
$c$	= velocity of light, m/s
$C_p$	= specific heat at constant pressure, J/kgK
$g$	= statistical weight
$h$	= Planck's constant, J.s
$h_0$	= specific total enthalpy, MJ/kg
$(h_0)_{av}$	= time averaged specific total enthalpy, MJ/kg
$h_{chem}$	= Chemical potential, MJ/kg
$I$	= probe laser intensity, $mW/mm^2$
$I_0$	= incident laser intensity, $mW/mm^2$
$k$	= absorption coefficient, $m^{-1}$
$k_B$	= Boltzmann constant, J/K
$K$	= integrated absorption coefficient, $GHz m^{-1}$
$M$	= Mach number

---

\* JSPS Research Fellow, Department of Aeronautics and Astronautics, matsui@al.t.u-tokyo.ac.jp. Member AIAA.

† Guest Associate Professor, Department of Advanced Energy, Member AIAA.

‡ Graduate student, Department of Aeronautics and Astronautics, Student Member AIAA.

§ Associate Professor, Department of Advanced Energy, Member AIAA.

\*\* Professor, Department of Aeronautics and Astronautics, Member AIAA.

†† President, Member AIAA.

$m$	=	mass of absorber, kg
$\dot{m}$	=	mass flow rate, g/s
$n$	=	number density, $m^{-3}$
$P$	=	Input power, kW
$p_{amb}$	=	ambient pressure, Pa
$p_{pitot}$	=	Pitot pressure, Pa
$p_{tube}$	=	tube pressure, Pa
$\dot{q}$	=	heat flux, $MW/m^2$
$r$	=	radial coordinate, mm
$R$	=	Gas constant, J/kgK
$T$	=	translational temperature, K
$t$	=	elapsed time, ms
$u$	=	flow velocity, m/s
$x$	=	coordinate in the laser pass direction, mm
$y$	=	probe beam position, mm
$\alpha_O$	=	degree of dissociation in oxygen
$\alpha_N$	=	degree of dissociation in nitrogen
$\gamma$	=	Specific heat ratio
$\Delta E$	=	energy gap, eV
$\lambda$	=	wavelength, nm
$\nu$	=	laser frequency, Hz
$\nu_0$	=	center absorption frequency, Hz
$\Delta \nu_D$	=	Doppler width, GHz
$\rho$	=	density, $kg/m^3$
$\tau$	=	plasma emitted duration, m

*Subscript*

$i$	=	absorption state
$j$	=	excited state

## I. Introduction

Development of thermal protection systems (TPS) requires the simulation of entry and re-entry conditions at ground test facilities. Arc-heaters are widely used to generate such high enthalpy flows because of their long operational time, simple structure and ease of maintenance.<sup>1-4</sup> However, surface catalytic effects and active and passive oxidation of TPS materials have been recognized as important issues<sup>5-8</sup>; erosion of their electrodes poses an important obstacle because polluted flows make it difficult to evaluate chemical reaction rates in front of TPS surfaces.<sup>9, 10</sup> For the reasons above, inductively coupled plasma generators have garnered much attention.<sup>11-13</sup> Such generators have no electrode. They can produce an ideal test condition for TPS tests because they have no undesirable chemical reactions that result from erosion. Another advantage of such generators is that they can use even reactive gases such as carbon dioxide and oxygen because of their electrode-less heating. Mars or Venus entry conditions can be simulated using these generators.<sup>14</sup>

An inductively heated plasma generator IPG3 was developed at the Institut für Raumfahrtssysteme at the University of Stuttgart.<sup>11, 14</sup> A schematic illustration of IPG3 and its power supply system are shown in Fig. 1. A Meissner type resonant circuit is used as a RF oscillator. Its operational frequency can be optimized to achieve high energy coupling efficiency for various gas species by switching the number of capacitors. Figure 2 shows the plasma emission signal measured by a photo detector. The signal has a specific fluctuation of 300 Hz. This fact implies that the flow generated by IPG3 is not stationary.

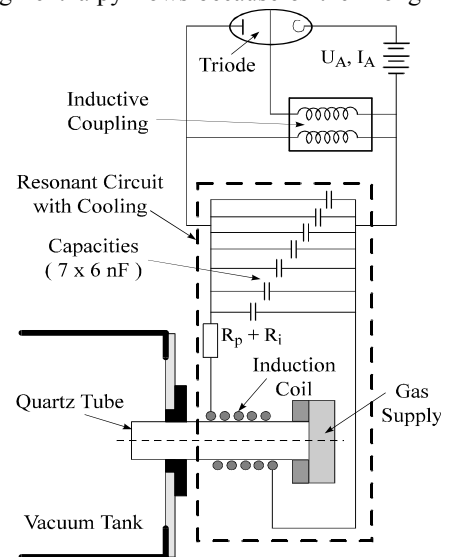


**Fig. 1 IPG3 and Meissner type resonant circuit.**

Various intrusive measurements using a calorimeter, Pitot probe, Mach probe, and heat flux probe have been applied to the flows.<sup>15, 16</sup> The operation condition and measured parameters by these methods are tabulated in Tables 1 and 2, respectively. Nevertheless, it is still difficult to measure temporal and spatial variations of flow properties, which would be valuable information for validation of intrusive measurements and further studies of TPS surface physics. In our previous study, laser absorption spectroscopy (LAS) was applied to pure oxygen flow generated by IPG3 and flow properties were successfully estimated.<sup>17</sup> In this study, LAS has been applied to air and nitrogen flows and the temporal and time-averaged specific enthalpy and degree of dissociation in oxygen and nitrogen were estimated.

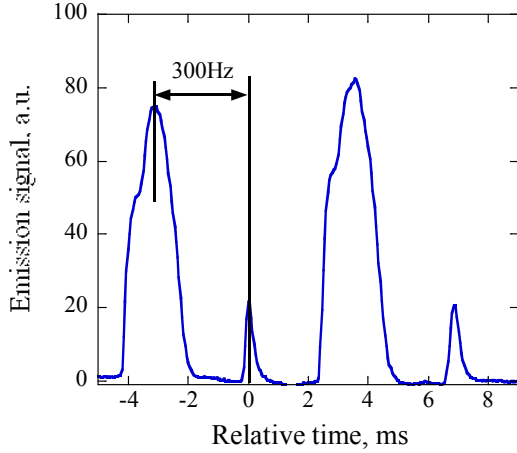


Fig. 2 Emission signal.

Table 1. Operational conditions

Operational condition	Air	N <sub>2</sub>
Mass flow $\dot{m}$	8 g/s	8 g/s
Anode Power $P$	125 kW	130 kW
RF frequency $f$	640 kHz	-
Ambient pressure $p_{amb}$	80 Pa	80 Pa

Table 2. Measured parameters in air flow

Parameter	Air
Plasma power $P_{plasma}$	28.2 kW
Pitot pressure $p_{pitot}$	380 Pa
Mach number $M$	1.94
Heat flux density $\dot{q}$	0.5 MW/m <sup>2</sup>
Specific enthalpy $h_0$	17.5 MJ/kg

## II. Theory of Laser Absorption Spectroscopy

Laser absorption spectroscopy has some superiority to other non-intrusive spectroscopes such as emission and LIF: 1) it is applicable to optically thick plasma, and 2) absolute calibration using a standard light source or a density reference cell is not necessary. Moreover, 3) the measurement system is portable when a diode laser is used. In our experimental conditions, Doppler broadening is several gigahertz, which is two orders of magnitude greater than all other broadenings, including natural, pressure and Stark broadenings. The absorption profile is approximated as a Gaussian profile, expressed as<sup>18-20</sup>

$$k(\nu) = \frac{2K}{\Delta\nu_D} \sqrt{\frac{\ln 2}{\pi}} \exp \left[ -\ln 2 \left\{ \frac{2(\nu - \nu_0)}{\Delta\nu_D} \right\}^2 \right]. \quad (1)$$

Here,  $\Delta\nu_D$  is related to the translational temperature  $T$ , expressed as,

$$\Delta\nu_D = 2\nu_0 \sqrt{\frac{2k_B T}{mc^2} \ln 2}. \quad (2)$$

The number density of absorbers is related to  $K$  as,

$$n_i = \frac{8\pi\nu_0^2}{c^2 A_{ji}} \frac{g_i}{g_j} K. \quad (3)$$

The target line is that of atomic oxygen at 777.19 nm (3s5S  $\rightarrow$  3s5P) and atomic nitrogen at 859.40 nm (3s2P  $\rightarrow$  3p2P).

### III. Experimental Setup

Figure 3 shows a schematic of the measurement system. A tunable diode-laser with an external cavity (Velocity Model 6300; New Focus Inc.) was used as the laser oscillator. Its line width was less than 300 kHz. The laser frequency was scanned over the absorption line shape  $k(\nu)$ . The modulation frequency and width were 1 Hz and 30 GHz, respectively. The laser intensity, which was normalized by saturation intensity<sup>20</sup>, was 0.08; it was sufficiently small to avoid the influence of absorption saturation.<sup>22</sup> An optical isolator was used to prevent the reflected laser beam from returning into the external cavity. An etalon was used as a wave-meter. Its free spectral range was 0.75 GHz.

The probe beam was guided to the chamber window through a multimode optical fiber. The fiber output was mounted on a one-dimensional traverse stage to scan the flow in the radial direction. The probe beam diameter was 2 mm at the chamber center. Transmitted laser intensity was measured at 3 m away from the plume to reduce plasma emission signal using a photo detector (DET110/M; Thorlabs Inc.) A parabola mirror allowed scanning of the plume without synchronizing the detector position with the probe beam position. Signals were recorded using a digital oscilloscope (NR-2000; Keyence Co.) with 14-bit resolution at the sampling rate of 20 kHz.

Figure 4 shows that the measured region was 140 mm downstream from the generator exit. Axisymmetric distributions of flow properties were assumed here. Table 1 shows operational conditions of the IPG3.

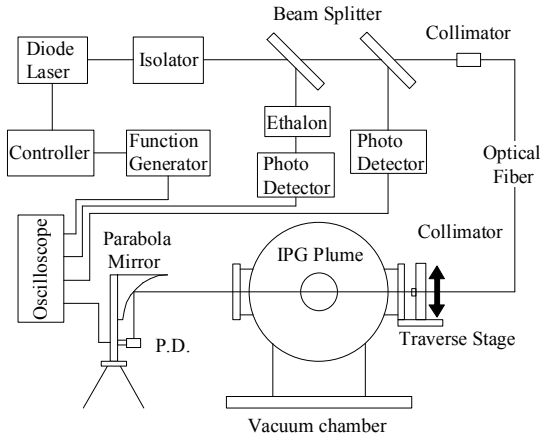


Fig. 3 Measurement system.

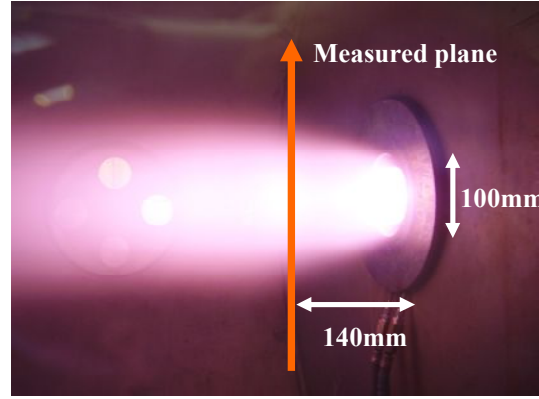


Fig. 4 A photograph of IPG3 air plume.

### IV. Results

#### A. Air Flow Diagnostics

Figure 5 shows the history of an absorbance  $-\ln(I/I_0)$  along with an emission signal. The absorbance fluctuated in synchronization with the emission signal with a duration  $\tau$  of 3.3 ms. The trace is regularly, and can be categorized into two modes as shown in Fig.5.

Typical signals that were recorded with frequency modulation are shown in Fig. 6 along with an etalon signal. We recorded 40 cycles of frequency modulation for each measurement position. In each cycle, the absorbance is extracted every 0.25 ms. Figure 7 shows typical absorbance that were extracted from the scanned absorption profile. Here, the origin of elapsed time,  $t=0$ , is set at the maximum signal in Mode 1. Then, we obtained a time-synchronous absorption profile by rearranging the absorbance according to the same elapsed time in the same Mode as shown in Fig.8.

Since the absorbance is path-integrated absorption coefficients, Abel inversion is applied to obtain absorption coefficients. Assuming axisymmetric distributions of flow properties, the absorption coefficient is obtained by the following Abel inversion as,

$$k(\nu) = \frac{1}{\pi} \int_r^R \frac{d \left( \ln \left( \frac{I}{I_0}(x, \nu) \right) \right) / dx}{\sqrt{x^2 - y^2}} dx \quad (4)$$

Since the absorption coefficients are dependent on the frequency, the Abel inversion should be conducted frequency by frequency. Here, after curve fitting to the path-integrated absorption profiles in Fig.8, the absorbance is extracted every 0.4 GHz from the fitted curves and then the absorption profile is obtained.

Figure 9 shows that the history of translational temperature, as deduced from line broadening of the absorption profiles, was almost constant of 3600 K, being different from the emission signal. On the other hand, as shown in Fig. 10, the history of number density of OI 3s5S shows the similar trace with the emission signal. The maximum number density was  $5 \times 10^{15} \text{m}^{-3}$ .

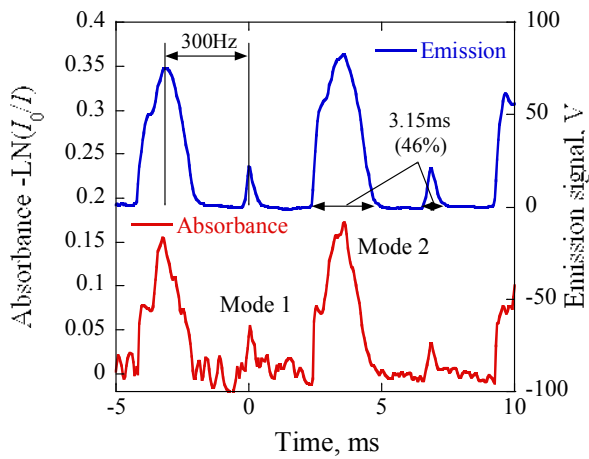


Fig. 5 Absorbance and emission signals.

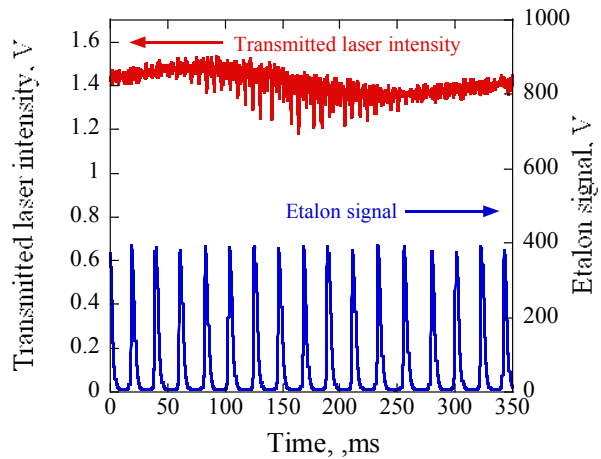


Fig. 6 Typical transmitted laser and etalon signals.

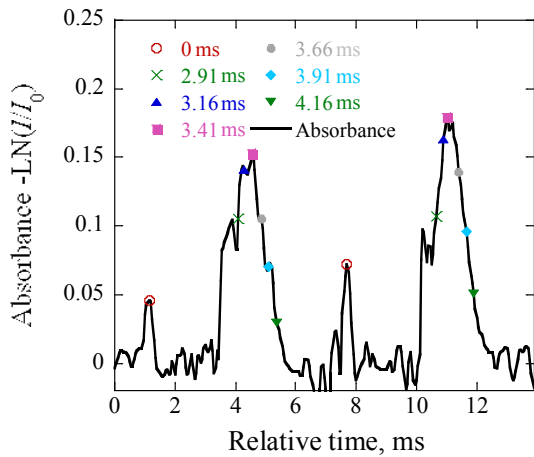


Fig. 7 Typical absorbance and extracted

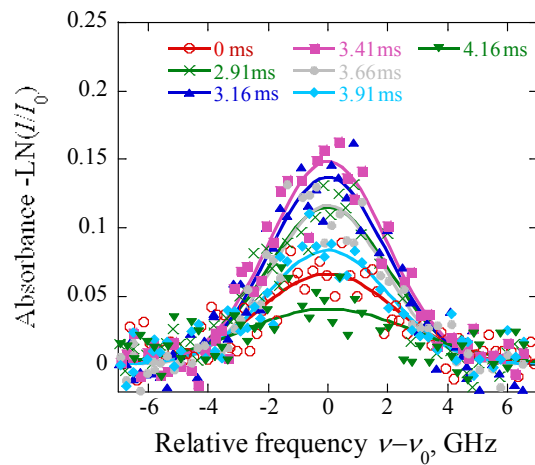
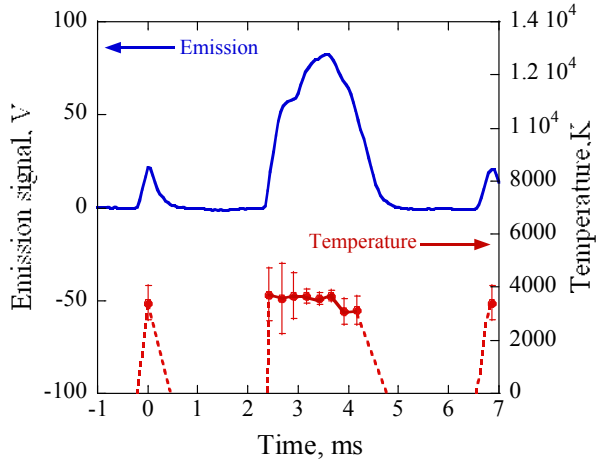
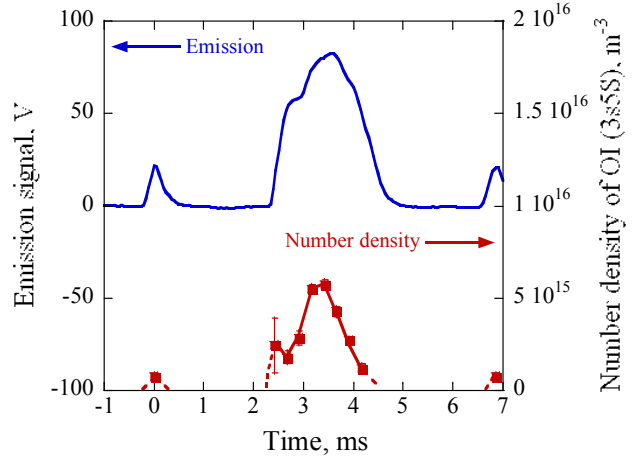


Fig. 8 Temporal variations of path-integrated



**Fig. 9 History of translational temperature and etalon signals.**



**Fig. 10 History of OI (3s5S) number density and etalon signals.**

### B. Nitrogen Flow Diagnostics

In this operation condition, the absorption signal of NI (3s2P) could not be detected. Because current limitation of the measurement system is the fractional absorption of 1%, the number density might be smaller than  $3.7 \times 10^{14} \text{ m}^{-3}$  assuming the temperature of 4000K.

## V. Discussion

### A. Temporal Variation of Specific enthalpy and Chemical Composition

The specific enthalpy and degree of dissociation in oxygen and nitrogen were estimated as follows. Assuming an isentropic expansion and chemically frozen flow through the nozzle, the total specific enthalpy is conserved, which fact is expressed as

$$h_0 = \int_0^{T_0} C_p dT' + h_{\text{chem}} = \int_0^T C_p dT' + h_{\text{chem}} + \frac{1}{2} u^2. \quad (5)$$

Here,  $h_{\text{chem}}$  is constant under the chemically frozen flow assumption and  $u$  is expressed as,

$$u = M \sqrt{\gamma R T}. \quad (6)$$

In this study,  $u$  is estimated from measured Mach number by the pitot probe and the temperature by LAS.

The total pressure measured in the discharge tube was as high as 11 kPa as tabulated in Table 2. Therefore, the chemical composition in the tube was calculated assuming thermo-chemical equilibrium. In that calculation, eleven chemical species were considered,  $\text{N}_2$ ,  $\text{O}_2$ ,  $\text{N}$ ,  $\text{O}$ ,  $\text{NO}$ ,  $\text{N}_2^+$ ,  $\text{O}_2^+$ ,  $\text{N}^+$ ,  $\text{O}^+$ ,  $\text{NO}^+$  and  $e^-$ . Their equilibrium constants were obtained from Refs 23. In addition,  $C_p$  was computed as the sum of the contributions of all species. Figure 11 shows the calculated mole fraction and specific enthalpy as a function of  $T_0$ .

Using Eq. (5), history of total temperature was deduced from the measured temperature and velocity. It was around from 5200 K to 6700 K.

Figure 12 show a history of specific total enthalpy and

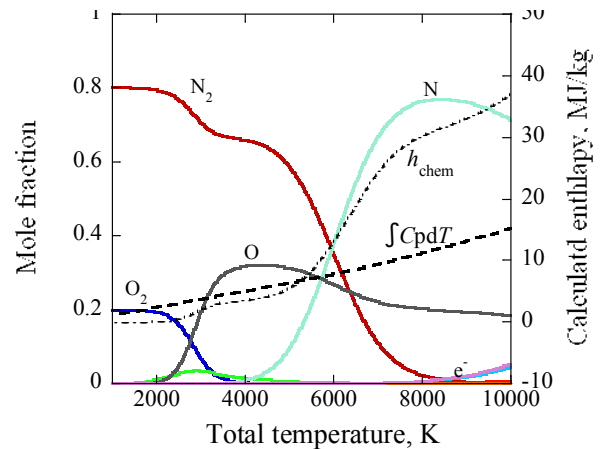


**Fig. 11 Calculated enthalpy and mole fractions by thermo-chemical equilibrium assumptions,  $p_{\text{tube}}=11 \text{ kPa}$ .**

the emission signal. The maximum specific total enthalpy was 30.3 MJ/kg.

Figure 13 shows a history of degree of dissociation in oxygen and nitrogen and the emission signal. Although the oxygen was almost fully dissociated, the degree of dissociation in nitrogen was around 50 %. In the measured temperature region, the degree of dissociation in nitrogen is very sensitive to the temperature variation. That's why the estimation error of the degree of dissociation in nitrogen and the specific total enthalpy were much larger than the measurement error of the temperature.

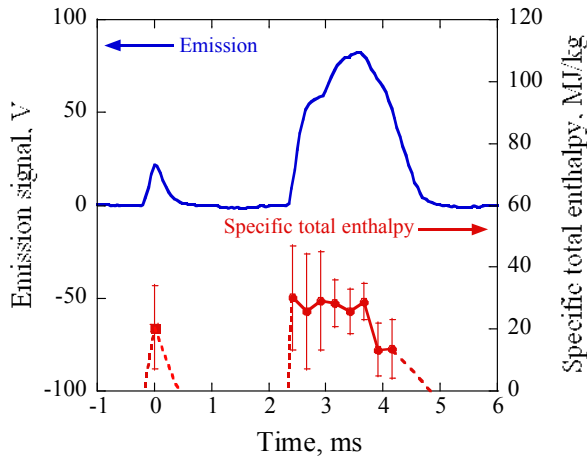


**Fig. 12 History of specific total enthalpy and emission signal.**

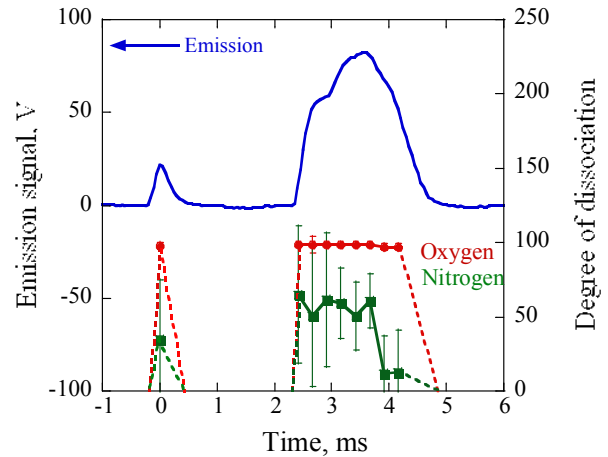


**Fig. 13 History of degree of dissociation in oxygen and nitrogen and emission signal.**

### B. Time-averaged Specific enthalpy and degree of dissociation

The time-averaged specific total enthalpy is defined as

$$(h_0)_{av} = \frac{\int_0^{\tau} h_0(t) \rho(t) u(t) dt}{\int_0^{\tau} \rho(t) u(t) dt} \quad (7)$$

However, the time-averaged specific total enthalpy in a whole cycle is difficult to estimate because of the uncertainty in the non-emitted time region. Assuming the temperature is room one of 300 K during the region, the time-averaged specific total enthalpy is estimated  $6.86 \pm 3.0$  MJ/kg, which might be much underestimated. Because the density is inversely proportional to the temperature, the influence of the high density during the room temperature region is significant. Practically, the gas in the region would be heated by conduction from before and after heated gas.

Here, the averaging was applied to the emitted duration time, which corresponds to 46% of the fluctuation cycle as shown in Fig.5. The estimated enthalpy, degree of dissociation in oxygen and nitrogen were  $23.5 \pm 10.1$  MJ/kg, 98% and 44%, respectively. Figure 14 shows the enthalpy balance, where chemical potential accounted for 66 % of the total specific enthalpy.

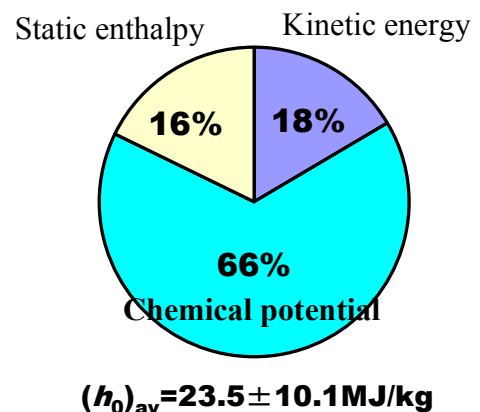


**Fig. 14 Enthalpy balance.**

## VI. Conclusion

Laser absorption spectroscopy was applied for the diagnostics of non-stationary IPG3 air and nitrogen flows. Consequently, in the air flow, temporal variation of the translational temperature and the number density of OI

(3s5S) were successfully measured though the absorption signal could not be detected in the nitrogen flow. The averaged total enthalpy, degree of dissociation in oxygen and nitrogen in the plasma emitted duration time of the air flow were estimated as  $23.5 \pm 10.1$  MJ/kg, 98% and 44 %, respectively.

### Acknowledgments

This work was partially supported by Research Fellowships of the Japan Society for the Promotion of Science for Young Scientists, 18-09885.

### References

- <sup>1</sup>Birkan, M. A., "Arcjets and Arc Heaters – An Overview of Research Status and Needs," *Journal of Propulsion and Power*, Vol. 12, No. 6, 1996, pp. 1011–1017.
- <sup>2</sup>Milos, F. S., "Flow Field Analysis for High-enthalpy Arc Heaters," *Journal of Thermophysics and Heat Transfer*, Vol. 6, No. 3, 1992, pp. 565–568.
- <sup>3</sup>Auweter-Kurtz, M., Kurtz, H. L., and Laure, S., "Plasma Generators for Reentry Simulation," *Journal of Propulsion and Power*, Vol. 12, No. 6, 1996, pp. 1053–1061.
- <sup>4</sup>Lago, V., Lebéhot, A., Dudeck, M., Pellerin, S., Renault, T., and Echegut, P., "Entry Conditions in Planetary Atmospheres: Emission Spectroscopy of Molecular Plasma Arcjets," *Journal of Thermophysics and Heat Transfer*, Vol. 15, No. 2, 2001, pp. 168–175.
- <sup>5</sup>Curry, D. M., Pham, V. T., Norman, I., and Chao, D. C., "Oxidation of Hypervelocity Impacted Reinforced Carbon," *Journal of Spacecraft and Rockets*, Vol. 37, No. 2, 2000, pp. 310–317.
- <sup>6</sup>Goulard, R., "On Catalytic Recombination Rates in Hypersonic Stagnation Heat Transfer," *Jet Propulsion*, Vol. 28, No. 11, 1958, pp. 737–745.
- <sup>7</sup>Balat, M. and Berjoan, R., "Oxidation of Sintered Silicon Carbide under Microwave-Induced CO<sub>2</sub> Plasma at High Temperature: Active-Passive Transition," *Journal of Applied Surface Science*, Vol. 161, 2000, pp. 434–442.
- <sup>8</sup>Bykova, N. G., Vasil'evskii, S. A., Gordeev, A. N., Kolesnikov, A. F., Pershin, I. S., and Yakushin, M. I., "Determination of the Effective Probabilities of Catalytic Reactions on the Surfaces on Heat Shield Materials in Dissociated Carbon Dioxide Flows," *Journal of Fluid Dynamics*, Vol. 32, No. 6, 1997, pp. 876–886.
- <sup>9</sup>Milos, F. S. and Shepard, C. E., "Thermal Analysis of an Arc-heater Electrode with a Rotating Arc Foot," *Journal of Thermophysics and Heat Transfer*, Vol. 8, No. 4, 1994, pp. 723–729.
- <sup>10</sup>Durgapal, P., "Electrode Phenomena in High-current, High-pressure Arc Heaters," *Journal of Thermophysics and Heat Transfer*, Vol. 7, No. 3, 1993, pp. 412–417.
- <sup>11</sup>Herdrich, G., Auweter-Kurtz, M., and Kurtz, H., "New Inductively Heated Plasma Source for Reentry Simulations," *Journal of Thermophysics and Heat Transfer*, Vol. 14, No. 2, 2000, pp. 244–249.
- <sup>12</sup>Bottin, B., Varbonaro, M., Van der Haegen, V., and Paris, S., "Predicted and Measured Capability of the VKI 1.2MW Plasmatron Regarding Re-entry Simulation," *ESA SP-426*, 1998, pp. 553–560.
- <sup>13</sup>Gordeev, A. N., "Overview of Characteristics and Experiments in IPM Plasmatrons," VKI, RTO AVT/VKI Special Course on "Measurement Techniques for High Enthalpy Plasma Flows," RTO EN-8, Rhode-Saint-Genesne, Belgium, Oct. 1999.
- <sup>14</sup>Herdrich, G., Auweter-Kurtz, M., Endlich, P., and Kurtz, H., "Mars Entry Simulation Using an Inductively Heated Plasma Generator," *Journal of Propulsion and Power*, Vol. 40, No. 5, 2003, pp. 690–693.
- <sup>15</sup>Herdrich, G., Auweter-Kurtz, M., Kurtz, H., Laux, T., and Winter, M., "Operational Behavior of Inductively Heated Plasma Source IPG3 for Entry Simulations," *Journal of Thermophysics and Heat Transfer*, Vol. 16, No. 3, 2002, pp. 440–449.
- <sup>16</sup>Herdrich, G. and Auweter-Kurtz, M., "Development and Characterization of Inductively Heated Plasma Generator for Atmospheric Entry Simulations," *AIAA Paper 04-2503*, Jun. 2004.
- <sup>17</sup>Matsui, M., Komurasaki, K., Herdrich, G., Auweter-Kurtz, M., "Enthalpy Measurement in Inductively Heated Plasma Generator Flow by Laser Absorption Spectroscopy," *AIAA Journal* Vol.43, No.9, 2005, pp.2060-2064
- <sup>18</sup>Baer, D. S., Nagali, V., Furlong, E., Hanson, R. K., and Newfield, M. E., "Scanned- and Fixed-wavelength Absorption Diagnostics for Combustion Measurements using Multiplexed Diode Lasers," *AIAA Journal*, Vol. 34 No. 3, 1996, pp. 489–493.
- <sup>19</sup>Matsui, M., Takayanagi, H., Oda, Y., Komurasaki, K., and Arakawa, Y., "Performance of arcjet-type atomic-oxygen generator by laser absorption spectroscopy and CFD analysis," *Vacuum*, Vol. 73, No. 3, 2004, pp. 341–346.
- <sup>20</sup>Yariv, A., "Quantum Electronics," second ed., Wiley, New York, 1975.
- <sup>21</sup>Park, C., "Nonequilibrium Hypersonic Aerothermodynamics," John Wiley and Sons, New York, 1990.
- <sup>22</sup>Matsui, M., Komurasaki, K., and Arakawa, Y., "Saturation absorption in laser absorption spectroscopy," *AIAA Paper 04-2597*, Jun. 2004.
- <sup>23</sup>Gupta, R. N., Yos, J. M., Thompson, R. A., and Lee, K. P., "A Review of Reaction Rates and Thermodynamic and Transport Properties for an 11-Species Air Model for Chemical and Thermal Nonequilibrium Calculations to 30000K," NASA Reference Publication 1232, 1990.